JOURNAL OF VIROLOGY, Sept. 1997, p. 6582–6592 Vol. 71, No. 9
0022-538X/97/$04.00+0

Membrane Binding of Human Immunodeficiency Virus Type 1 Matrix Protein In Vivo Supports a Conformational Myristyl Switch Mechanism

PAUL SPEARMAN,[1]* ROBERT HORTON,[2] LEE RATNER,[2] AND IRINA KULI-ZADE[1]

Departments of Pediatrics and Microbiology and Immunology, Vanderbilt University School of Medicine, Nashville, Tennessee 37232-2581,[1] and Division of Molecular Oncology, Washington University School of Medicine, St. Louis, Missouri 63110[2]

Received 17 January 1997/Accepted 30 May 1997

The interaction of the human immunodeficiency virus (HIV) Gag protein with the plasma membrane of a cell is a critical event in the assembly of HIV particles. The matrix protein region (MA) of HIV type 1 (HIV-1) $Pr55^{Gag}$ has previously been demonstrated to confer membrane-binding properties on the precursor polyprotein. Both the myristic acid moiety and additional determinants within MA are essential for plasma membrane binding and subsequent particle formation. In this study, we demonstrated the myristylation-dependent membrane interaction of MA in an in vivo membrane-binding assay. When expressed within mammalian cells, MA was found both in association with cellular membranes and in a membrane-free form. In contrast, the intact precursor $Pr55^{Gag}$ molecule analyzed in an identical manner was found almost exclusively bound to membranes. Both membrane-bound and membrane-free forms of MA were myristylated and phosphorylated. Differential membrane binding was not due to the formation of multimers, as dimeric and trimeric forms of MA were also found in both membrane-bound and membrane-free fractions. To define the requirements for membrane binding of MA, we analyzed the membrane binding of a series of MA deletion mutants. Surprisingly, deletions within alpha-helical regions forming the globular head of MA led to a dramatic increase in overall membrane binding. The stability of the MA-membrane interaction was not affected by these deletions, and no deletion eliminated membrane binding of the molecule. These results establish that myristic acid is a primary determinant of the stability of the Gag protein-membrane interaction and provide support for the hypothesis that a significant proportion of HIV-1 MA molecules may adopt a conformation in which myristic acid is hidden and unavailable for membrane interaction.

Retroviral particle assembly is directed by the products of the *gag* gene. The *gag* gene of human immunodeficiency virus type 1 (HIV-1) encodes a 55-kDa precursor molecule ($Pr55^{Gag}$) which is sufficient for particle assembly in a variety of cell types (21, 22, 31). $Pr55^{Gag}$ molecules are produced from the unspliced genomic RNA on free ribosomes in the cytoplasm of infected cells (37) and are transported via an unknown mechanism to the plasma membrane. $Pr55^{Gag}$ molecules then interact specifically with the plasma membrane and with each other to form budding particles. During and immediately following budding, the HIV protease cleaves $Pr55^{Gag}$ into four major cleavage products: matrix (MA), capsid (CA), nucleocapsid (NC), and p6.

The cotranslational addition of the 14-carbon fatty acid myristic acid to the N-terminal glycine residue of $Pr55^{Gag}$ is essential for the plasma membrane targeting and binding functions of the molecule (5, 19, 34). Analysis of Gag protein mutants has suggested that domains within the N-terminal MA region of $Pr55^{Gag}$ but distinct from the myristylation site also play a role in plasma membrane targeting and binding (34, 41, 42). In addition to its central role in promoting an interaction with the plasma membrane, other functions which have been attributed to the MA region of HIV-1 $Pr55^{Gag}$ include incorporation of the viral envelope protein onto the developing particle (12, 15, 40), an essential role in early postentry events of the viral life cycle (39), nuclear targeting of the viral preintegration complex (7, 16–18, 36), and a role in particle assembly and budding through the formation of MA-MA multimers (23).

The function of Gag proteolytic cleavage products such as MA may differ markedly from the function of the same regions within the uncleaved precursor molecule. For example, a positively charged region within the N-terminal portion of HIV-1 MA contributes to plasma membrane transport and binding during particle assembly but can also direct the transport of heterologous proteins to the nucleus of the cell. In nondividing cells such as terminally differentiated macrophages, the nuclear targeting role of this MA domain is essential for transport of the viral preintegration complex to the nucleus (7, 17). Such a dual targeting role requires that MA be capable of regulated association and dissociation from the plasma membrane. Identification of the regulatory mechanisms underlying the reversal of membrane binding of MA would be beneficial to an understanding of both assembly and postentry steps in the virus life cycle and could lead to unique opportunities for the development of antiviral therapies.

The crystal structure of MA provides a compelling model for the MA-plasma membrane interaction (20). The MA monomer consists of five alpha helices, four of which pack tightly together to form the globular "head" of the molecule, while a C-terminal alpha helix (helix 5) projects away from the packed helical bundle. The crystal structure revealed a trimeric complex with a putative membrane-binding interface along one surface of the globular domain which contains four exposed

* Corresponding author. Mailing address: Departments of Pediatrics and Microbiology and Immunology, Vanderbilt University School of Medicine, D-7235 Medical Center North, Nashville, TN 37232-2581. Phone: (615) 322-2250. Fax: (615) 343-9723. E-mail: paul.spearman@mcmail.vanderbilt.edu.

basic residues (Lys-26, Lys-27, Lys-30, and Lys-32). According to this model, myristate inserts into the lipid bilayer while ionic bonds between the exposed lysine residues and acidic phospholipid head groups of the inner surface of the bilayer strengthen the interaction. The model is supported by the observation that mutagenesis of the four exposed lysine residues within a proviral clone decreased viral particle production from transfected HeLa cells (14). However, this model does not suggest how the dissociation of MA from cellular membranes occurs. In addition, the actual position of the myristate moiety in the molecule was not determined by X-ray crystallography, as the crystallized recombinant protein was not myristylated.

Zhou and Resh have recently proposed a model for the reversible membrane interaction of HIV-1 Gag proteins with the plasma membrane in which the myristylated N terminus of MA may adopt a hidden, membrane-inaccessible conformation (43). By using an in vitro membrane-binding assay, they found that the C-terminal alpha helix (helix 5) may act to inhibit membrane interactions by sequestering the myristylated N terminus within the molecule and away from the membrane-binding interface.

To further define the membrane-binding properties of the HIV MA protein, we have employed an in vivo membrane-binding assay using equilibrium flotation centrifugation. The utility of this assay in differentiating membrane-bound from membrane-free proteins was demonstrated by using myristylated MA and nonmyristylated MA, as well as other proteins whose intracellular distribution is known. Myristylated MA within cells was found in membrane-bound and membrane-free forms, while nonmyristylated MA was entirely membrane free. The proportion of membrane-free MA was markedly higher than that of myristylated $Pr55^{Gag}$, a difference which was not due to inefficient myristylation or to the inability of MA in either compartment to form oligomers. Phosphorylated MA was observed in both membrane-bound and membrane-free compartments. By using a panel of MA deletion constructs, we found that disruption of alpha-helical structure regions within the globular head of the molecule dramatically increased the membrane binding of MA. These data support a myristyl switch mechanism of reversible membrane binding of MA in which the myristyl group is hidden within the globular head of the molecule and may become accessible for membrane interactions upon an alteration in protein conformation.

MATERIALS AND METHODS

Cells and viruses. BSC-40 (African green monkey kidney) cells were maintained in Dulbecco's modified Eagle medium (DMEM; Atlanta Biologicals, Atlanta, Ga.) supplemented with 10% fetal bovine serum, 100 U of penicillin per ml, and 100 μg of streptomycin per ml at 37°C in 5% CO_2. H9/IIIB cells were obtained from R. Gallo through the National Institutes of Health (NIH) AIDS Research and Reference Reagent Program and maintained in RPMI 1640 medium (Atlanta Biologicals) supplemented with 10% fetal bovine serum, 100 U of penicillin per ml, and 100 μg of streptomycin per ml at 37°C in 5% CO_2. Recombinant vaccinia virus VTF 7-3 was obtained from T. Fuerst and B. Moss through the NIH AIDS Research and Reference Reagent Program.

Plasmid construction. pTM1 or pTM3 (24) was employed as the expression plasmid for wild-type MA, Myr-MA, and an MA region deletion construct panel designated MAD-1 to MAD-10. All MA sequences were cloned into the *Nco*I and *Bam*HI sites of the polylinker region, in the correct orientation with respect to the T7 promoter. PCR cloning was used to introduce an *Nco*I site at the ATG start codon for MA and a stop codon followed by a *Bam*HI site following the tyrosine 132 codon of MA. The following primers were used for MA sequence amplification. *Nco*I primer 1 (wild-type sequence and pMAD constructs), AGAGCCATGGGTGCGAGAGCGTCAGTA; *Bam*HI primer, CGGGAT CCTTAGTAATTTTGGCTGACCTGATT. To introduce a glycine 2-to-alanine 2 mutation in the Myr-MA construct, the following primer was substituted for *Nco*I primer 1: *Nco*I primer 2 (Myr-MA only), AGAGCCATGGCTG CGAGAGCGTCAGTA. The template for PCR cloning of wild-type MA and Myr-MA was pHXB2gpt2 (29). The template for cloning of MA deletion constructs MAD-1 to MAD-10 was a previously described panel of deletion mutants from the laboratory of Max Essex (39, 40). The designation formerly used by his laboratory (D1 to D10) corresponds to MAD-1 to MAD-10 in this report; i.e., D1 is MAD-1, D2 is MAD-2, etc. A schematic diagram of the deletion constructs is included in Fig. 1. Each construct was verified by restriction digest analysis and DNA sequencing. The plasmids used for expression of HIV $Pr55^{Gag}$ (p55G1) and gp160 (HX) and *Escherichia coli* β-galactosidase (pTM/LacZ) with the vaccinia virus/T7 system have been previously described (9, 34).

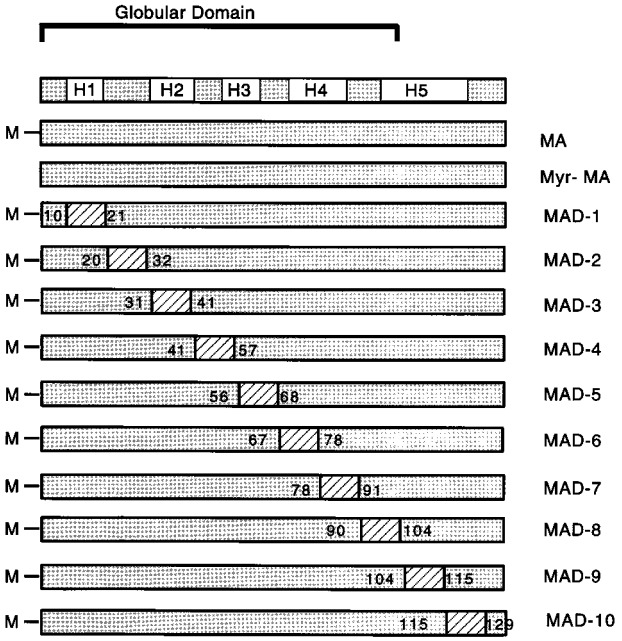

FIG. 1. Schematic representation of MA expression constructs. At the top is a representation of the five alpha helices (H1 to H5) of MA as defined by the crystal structure. Hatched regions represent deleted regions in pMAD1 to pMAD10, and the bordering intact residues are indicated. Numbering for HXB2 MA residues is given starting from the initiator methionine residue (methionine 1). M denotes an intact myristylation site.

Expression with the vaccinia virus/T7 RNA polymerase expression system and metabolic labelling of Gag protein. BSC-40 cells (10^6) were seeded the night before each experiment onto 100-mm^2 dishes. Cells were infected with 10 PFU of recombinant vaccinia virus VTF 7-3 per cell and then transfected 30 min later with cesium chloride-purified plasmid DNA by cationic liposome-mediated transfection with dimethyldioctadecylammonium bromide (30). The medium was removed 6 h posttransfection and replaced with DMEM deficient in leucine (GIBCO BRL, Gaithersburg, Md.). After 30 min, cells were washed and fresh medium deficient in leucine but supplemented with 100 μCi of [^{3}H]leucine per ml. Labelling was carried out for 1 h, after which the medium was replaced with complete DMEM. Following an additional 1 h of incubation, cells were collected and processed as described below. In some experiments, 100 μCi of [^{3}H]myristic acid per ml in DMEM with 10% fetal calf serum depleted of lipids was used in place of [^{3}H]leucine-containing medium and labelling was carried out for a total of 4 h. Similarly, in some experiments the cells were labelled for 4 h with 200 μCi of [^{32}P]orthophosphate in phosphate-deficient RPMI medium prior to processing.

Equilibrium flotation centrifugation with membranes. A flotation method for the analysis of membrane-bound proteins has been previously described and applied to the analysis of vesicular stomatitis virus MA protein (10, 11). This procedure was utilized in our experiments with only minor modifications. Metabolic labelling of cells expressing Gag protein was carried out 6 h posttransfection as described above. Following the 1-h labelling and 1-h chase periods, cells were collected by scraping, washed twice in NTE buffer (100 mM NaCl, 10 mM Tris [pH 7.4], 1 mM EDTA), and suspended for 10 min in hypotonic medium (10 mM Tris [pH 7.4], 1 mM EDTA, antipain at 1 μg/ml, aprotinin at 5 μg/ml, leupeptin at 1 μg/ml, pepstatin at 1 μg/ml, 1 mM phenylmethylsulfonyl fluoride). Lysis was carried out by gentle Dounce homogenization (10 to 20 strokes), monitored by phase-contrast microscopy, and terminated upon lysis of 85 to 90% of cells. The solution was then adjusted to 150 mM NaCl–1 mM $MgCl_2$ and centrifuged at 1,000 × *g* for 10 min at 4°C to remove nuclei and unbroken cells. The resulting supernatant (S1) was adjusted to 80% sucrose and layered at the bottom of an 80%-65%-10% sucrose step gradient in NTE buffer. Standard volumes for this step gradient included 1.5 ml of 80% sucrose and 6 ml of 65%

sucrose, and the remaining portion of the centrifuge tube was filled with 10% sucrose. Centrifugation was performed in a Beckman SW41 Ti rotor at 35,000 rpm for 18 h. Ten 1-ml fractions were collected from the bottom of the gradient, and the refractive index of each fraction was measured to determine the 65%-10% interface. For selected experiments, 5′ nucleotidase activity in each fraction was measured by using reagents from a commercial kit (Sigma Chemical Co., St. Louis, Mo.). When a second flotation gradient was used, 50% of the membrane-containing fractions from the first gradient was saved for detection of relevant proteins, while the remaining 50% was pooled, adjusted to 80% sucrose and 1 M NaCl, and loaded on the bottom of a second step gradient. Gag proteins in each fraction were immunoprecipitated by using pooled sera of HIV patients and analyzed via sodium dodecyl sulfate-polyacrylamide gel electrophoresis (SDS-PAGE) and fluorography using Amplify as the scintillant (Amersham, Arlington Heights, Ill.). Phosphorylation experiments were performed in a similar manner, with the addition of phosphatase inhibitors (final concentrations of 10 mM sodium fluoride, 200 μM sodium orthovanadate, and 5 mM sodium pyrophosphate) and analysis of immunoprecipitated proteins by SDS-PAGE and autoradiography. Experiments in which HIV gp160 or β-galactosidase was expressed utilized 100 μCi of [^{35}S]cysteine-methionine (ICN, Irvine, Calif.) per ml in DMEM deficient in cysteine and methionine (GIBCO). Immunoprecipitation of β-galactosidase from gradient fractions was carried out with an anti-β-galactosidase monoclonal antibody (Promega, Madison, Wis.). When indicated, Western blotting of immunoprecipitated Gag protein was performed by using anti-MA monoclonal antibodies (G11G1 and G11H3 [32], provided by A. Pinter, Public Health Research Institute, New York, N.Y.) and enhanced chemiluminescence detection methods (Amersham). Quantitation of immunoprecipitated protein bands on autoradiograms was performed by using NIH Image software (version 1.60).

Protease sensitivity analysis of membrane-bound Gag proteins. Gag proteins were produced and subjected to equilibrium flotation centrifugation as described above. Peak membrane-containing fractions from the gradient were pooled, diluted in phosphate-buffered saline (PBS), and subjected to centrifugation at 150,000 × *g* for 60 min at 4°C. The resulting membrane pellet was resuspended in PBS and divided into four equal aliquots. The aliquots were incubated at room temperature for 30 min together with (i) no additives, (ii) 200 μg of trypsin per ml, (iii) 1% Triton X-100, or (iv) 200 μg of trypsin per ml–1% Triton X-100. Each sample was placed on ice immediately following the incubation period, and protease inhibitors were then added. Analysis was performed by immunoprecipitation with sera from HIV patients, followed by immunoblotting by using pooled anti-MA monoclonal antibodies (for MA and Pr55^{Gag}) or an anti-p24 monoclonal antibody (C304; Tanox Biosystems, Houston, Tex.; used for detection of p24 from HIV-1 particles) and enhanced chemiluminescence detection methods. Control reactions were performed by utilizing HIV-1 virions which were purified from 38 ml of H9/HTLV-IIIB supernatant by filtration through a 0.45-μm-pore-size filter, followed by pelleting through a 20% sucrose cushion. The virion pellet was resuspended in PBS prior to aliquoting and treatment with regimens i to iv described above.

Differential sedimentation analysis. Differential sedimentation centrifugation of S1 fractions was carried out exactly as previously described (34). No detergents were utilized prior to sedimentation. Analysis of Gag protein in supernatant (S100) and pellet (P100) fractions was performed by Western blotting with anti-MA monoclonal antibodies. Detection was done via enhanced chemiluminescence detection methods.

Chemical cross-linking with glutaraldehyde. MA proteins were separated by equilibrium flotation centrifugation as described above, and 1-ml gradient fractions were collected. Each fraction was adjusted to 1% glutaraldehyde, starting from a 25% (wt/vol) stock. After 15 min of incubation on ice, 1 μl of a 10% sodium deoxycholate stock solution was added and ice-cold trichloroacetic acid (TCA) was added to achieve a 5% final concentration. TCA-precipitated protein was collected by centrifugation in a refrigerated microcentrifuge and washed in ice-cold acetone prior to resuspension in SDS-PAGE loading buffer. Samples were analyzed by SDS-PAGE and Western blotting with anti-MA monoclonal antibodies and enhanced chemiluminescence detection methods.

Immunofluorescence microscopy. BSC-40 cells were seeded onto glass coverslips the night before the experiment. Infection-transfection with VTF7-3 and Gag expression plasmids was performed exactly as described above. Cells were prepared for immunostaining 7 h posttransfection by washing with PBS and fixation with 50% methanol–50% acetone for 2 min. Antibody staining was performed by using anti-MA monoclonal antibodies G11G1 and G11H3, followed by a fluorescein isothiocyanate-conjugated anti-rat immunoglobulin G antibody. Cells were examined and photographed by using a Leitz Orthoplan microscope equipped for fluorescence under the 100× or 40× oil immersion objective.

RESULTS

Equilibrium flotation centrifugation reveals stable membrane binding of HIV-1 Pr55^{Gag}. To examine the membrane-binding characteristics of HIV-1 Gag proteins in vivo, we utilized equilibrium flotation centrifugation with membranes.

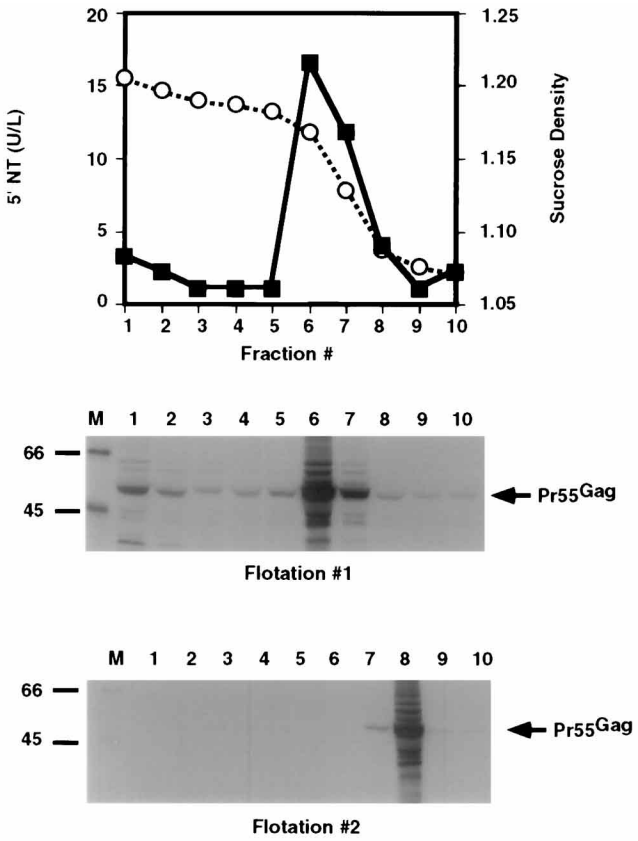

FIG. 2. Equilibrium flotation centrifugation of Pr55^{Gag}. Equilibrium flotation centrifugation of lysates from cells expressing Pr55^{Gag} was performed as described in the text. In the graph at the top, sucrose density in grams per milliliter (open circles) is plotted versus 5′ nucleotidase activity in units per liter (closed squares). Gradient fractions are indicated; the numbering represents equal fractions collected from the bottom (fraction 1) to the top (fraction 10). The corresponding autoradiogram of immunoprecipitated Pr55^{Gag} is shown below the graph (flotation 1). Gradient fractions surrounding the peak of membrane enzyme activity (fractions 5, 6, and 7) were pooled, adjusted to 1 M NaCl, and analyzed on a second equilibrium flotation gradient (flotation 2, bottom autoradiogram). Molecular masses are indicated in kilodaltons at the left. Lane M, marker lane.

This approach avoids potential problems associated with differential sedimentation in which insoluble aggregates may sediment with the membrane-enriched pellet and obviates the need for any detergent in the assay. In this assay, cell lysates with nuclei removed (S1 supernatants) are layered at the bottom of a sucrose step gradient and centrifuged to equilibrium. Cellular membranes rise to a sucrose interface, and membrane-associated proteins are readily identified at this interface when fractions are collected and analyzed.

Results of equilibrium flotation centrifugation of HIV-1 Pr55^{Gag} are shown in Fig. 2. The sucrose density interface containing cellular membranes is marked by the drop in sucrose density from fraction 6 to fraction 8 of the gradient (graph, open circles). A plasma membrane marker, 5′ nucleotidase, peaked in these fractions (closed squares). This demonstrates that cellular membranes are concentrated at the 65%-10% sucrose interface, allowing localization of the membrane-containing fractions of each gradient through determination of the sucrose density. HIV-1 Pr55^{Gag} was found to a large degree in the membrane-containing fractions of the gradient (Fig. 2, flotation 1). In repeated experiments, >90% of

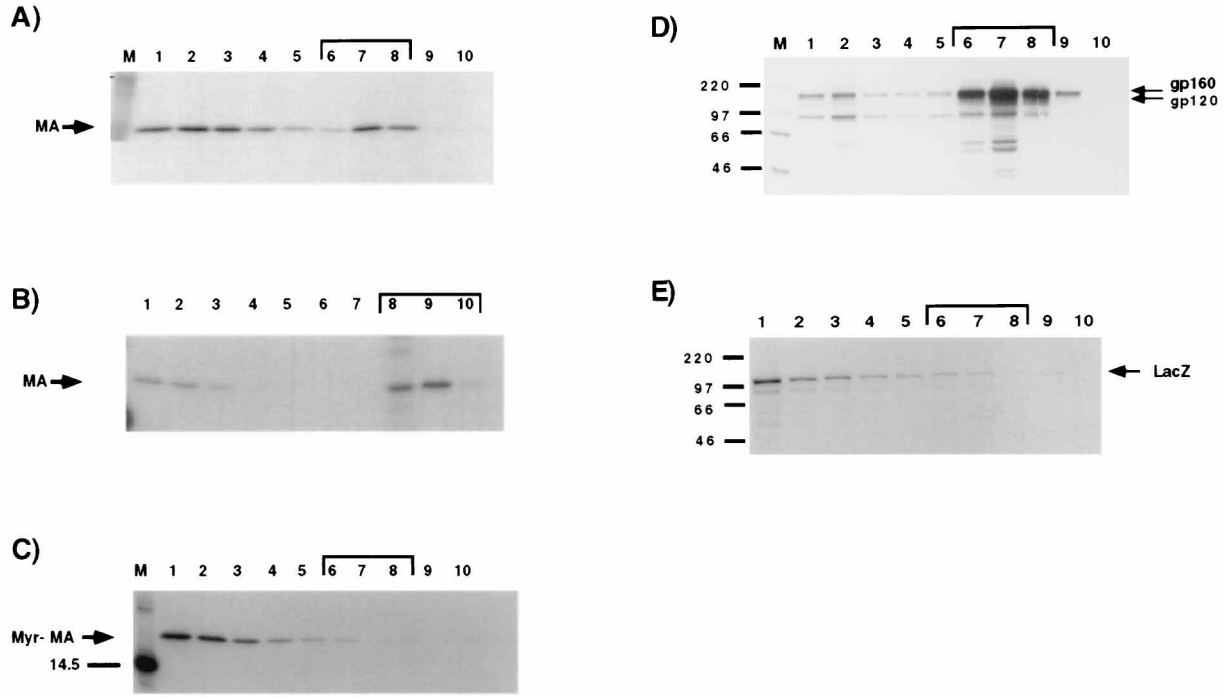

FIG. 3. Equilibrium flotation centrifugation of HIV MA protein. (A) HIV-1 MA protein was produced in BSC-40 cells, labelled with [^{3}H]leucine for 1 h, and chased for 1 h. Equilibrium flotation centrifugation was performed, and fractions were collected and immunoprecipitated with pooled sera from HIV patients as described in the text. Brackets indicate fractions with peak membrane content as determined by sucrose density identification of the 65%-10% interface. (B) Bracketed fractions from autoradiogram A were pooled, adjusted to 1 M NaCl, and subjected to equilibrium flotation centrifugation, followed by analysis as before. (C) HIV-1 MA protein containing a glycine 2-to-alanine mutation was expressed, labelled, and analyzed as in autoradiogram A. (D) HIV-1 envelope glycoprotein gp160 was expressed in BSC-40 cells, labelled with [^{35}S]cysteine-methionine, and subjected to analysis via equilibrium flotation centrifugation. Fractions collected and immunoprecipitated with sera from HIV patients were examined by SDS-PAGE and autoradiography. (E) *E. coli* β-galactosidase protein was expressed in BSC-40 cells, labelled with [^{35}S]cysteine-methionine, and analyzed by equilibrium flotation centrifugation. Detection was performed via immunoprecipitation with an anti-β-galactosidase monoclonal antibody (Promega), followed by SDS-PAGE and autoradiography. Molecular masses in kilodaltons are shown to the left of autoradiograms C, D, and E.

$Pr55^{Gag}$ was found associated with membranes by this method. We next assessed the stability of the Gag protein-membrane interaction to treatment with 1 M NaCl. This approach has previously been used to separate the weak electrostatic interactions demonstrated by some peripheral membrane proteins from the more stable interactions demonstrated by integral membrane proteins, viral MA proteins, and myristylated Gag proteins (5, 11, 34). Fractions 6, 7, and 8 were pooled, adjusted to 1 M NaCl, and subjected to a second equilibrium flotation centrifugation step. No Gag protein was dissociated from the membrane by this treatment (Fig. 2, flotation 2), indicating that this myristylated protein interacts in a stable manner with cellular membranes. The shift in the membrane fractions toward the top of the gradient demonstrated in this autoradiogram is explained by the increased volume loaded at the bottom of the gradient from the three pooled fractions of the first gradient.

Membrane binding of MA is less complete than that of $Pr55^{Gag}$ but demonstrates myristylation-dependent stability of binding. The membrane binding of HIV-1 MA was next examined by using equilibrium flotation centrifugation. In contrast to the results obtained with $Pr55^{Gag}$, more than one-half of the MA remained unbound to cellular membranes (Fig. 3A). Quantitation of the proportion of membrane-bound MA by densitometry following 1 h of labelling and a 1-h chase period revealed a mean of 33% membrane-bound protein (a result of three independent experiments). The stability of the interaction of MA with membranes was next assessed by pooling the membrane-containing fractions, adjusting them to a 1 M NaCl concentration, and performing a second equilibrium flotation centrifugation step. The interaction was stable when subjected to this treatment, with only a minor proportion of MA dissociated (Fig. 3B). Thus, the stability of the MA-membrane interaction is similar to that of $Pr55^{Gag}$, although the initial proportion of MA bound to membranes is much smaller.

We have previously demonstrated that a glycine 2-to-alanine mutation eliminates myristylation of $Pr55^{Gag}$ and of cleavage product MA (5, 34). We introduced this mutation into a plasmid construct expressing MA (Myr-MA) and analyzed the membrane binding of the nonmyristylated product by equilibrium flotation centrifugation. Myr-MA was found exclusively in the membrane-free fractions of the gradient (Fig. 3C). This established that the membrane binding of MA demonstrated in Fig. 3A and B is dependent upon myristylation. As additional validation of the ability of this assay to separate membrane-bound from cytosolic proteins, we examined the fractionation of HIV gp160, a membrane-bound protein, and of *E. coli* β-galactosidase, a cytosolic protein. The membrane association of gp160 was demonstrated (Fig. 3D), and the appearance of β-galactosidase in the bottom of the gradient was consistent with a membrane-free or cytosolic protein (Fig. 3E).

Gag proteins bound to membranes are not protected from proteolytic digestion. To validate the use of the high-ionic-strength buffer treatment used in the experiments described above, it was necessary to establish that the membrane-bound Gag proteins were accessible to the solution and did not reside in a protected environment inside of membrane vesicles. For this purpose, the membrane-containing fractions of equilib-

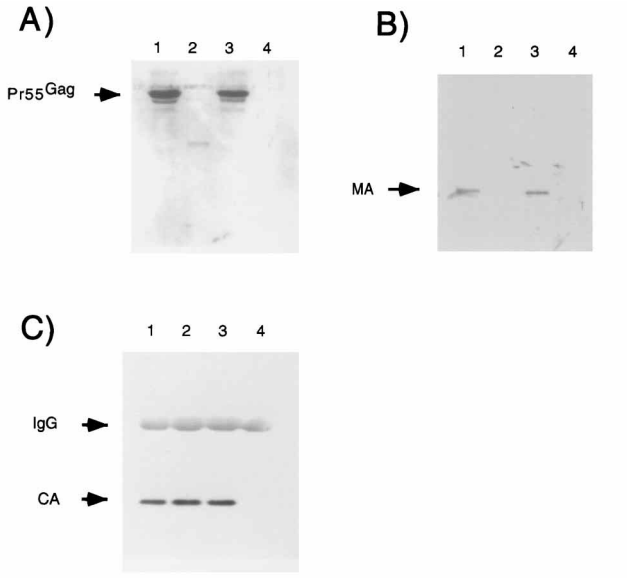

FIG. 4. Protease sensitivity of membrane-bound Gag proteins. Membrane preparations and HIV-1 virion particles were prepared as described in the text and incubated at room temperature with no additives (lane 1), trypsin at 200 μg/ml (lane 2), 1% Triton X-100 (lane 3), or trypsin plus Triton X-100 (lane 4). Detection was performed by Western blotting following immunoprecipitation with sera from HIV patients. A, $Pr55^{Gag}$; B, MA; C, HIV-1 virions; CA, capsid protein; IgG, immunoglobulin heavy chain from the immunoprecipitation procedure.

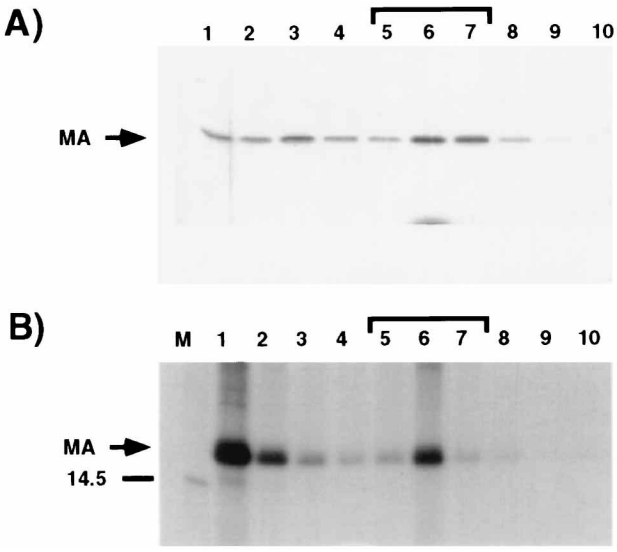

FIG. 5. Membrane association of myristylated MA and phosphorylated MA. (A) Cells were labelled with [^{3}H]myristic acid for 4 h prior to lysis and equilibrium flotation centrifugation. Analysis was done via immunoprecipitation with pooled sera from HIV patients and autoradiography. The brackets denote the 65%-10% sucrose interface of the gradient containing cellular membranes. (B) The HIV-1 MA protein was labelled with [^{32}P]orthophosphate for 4 h prior to equilibrium flotation centrifugation. Analysis was performed precisely as in autoradiogram A with the inclusion of phosphatase inhibitors.

rium flotation experiments were pooled and the membranes were subsequently pelleted. All of the membrane-bound Gag protein was found in the pelletable fraction (data not shown). The resuspended membranes and associated Gag proteins were then subjected to digestion with trypsin in the presence or absence of detergent, followed by immunoprecipitation and detection via Western blotting. $Pr55^{Gag}$ and MA were completely digested both in the presence (Fig. 4A and B, lane 4) and in the absence (Fig. 4A and B, lane 2) of detergent. In the control reaction, CA within HIV-1 IIIB virions was protected from proteolytic digestion in the absence of detergent (Fig. 4C, lane 2). These data support the accessibility of the membrane-bound Gag protein to trypsin and thus to the salt conditions employed in our flotation assay.

Differential membrane binding of MA is not due solely to myristylation or phosphorylation. Cotranslational modification with myristic acid or posttranslational modification via phosphorylation may influence the subcellular distribution of proteins. Because we observed MA in both membrane-free and membrane-bound forms by equilibrium flotation analysis (Fig. 3A), we asked whether incomplete myristylation may account for the appearance of MA in membrane-free fractions. MA was expressed as before and labelled for 4 h with [^{3}H]myristic acid prior to the membrane flotation procedure. ^{3}H-labelled MA was demonstrated in both the membrane-free and the membrane-containing fractions of the gradient. A parallel experiment in which Myr-MA was expressed revealed no labelling under these conditions, proving that the labelling seen in Fig. 5A is true myristylation and not nonspecific labelling of unmyristylated protein (data not shown). Next, we asked if differential phosphorylation of MA could explain the appearance of membrane-bound and membrane-free MA. MA was expressed as before, labelled with [^{32}P]orthophosphate for 4 h, and analyzed for membrane binding by flotation centrifugation. Phosphorylated MA was found in both membrane-containing and membrane-free fractions of the gradient (Fig. 5B). The distribution of MA bound to membranes versus that of membrane-free MA in this experiment was remarkably similar to that of MA labelled with [^{3}H]leucine (compare to Fig. 3A). Although these data do not establish whether phosphorylation at distinct residues plays a role in regulating the differential membrane binding of MA (see Discussion), they establish that phosphorylated MA and myristylated MA exist in both membrane-bound and membrane-free forms.

Multimeric MA is found in membrane-bound and membrane-free forms within cells. Crystallization of MA has revealed a trimeric structure (20). The biological significance of MA trimerization is not known, although there is some evidence that MA multimerization is essential to particle formation by $Pr55^{Gag}$ (23). We next examined MA separated by equilibrium flotation for the presence of multimers. MA was expressed and separated into membrane-bound and membrane-free fractions as before. Glutaraldehyde (1%) was employed as a chemical cross-linking agent as described in Materials and Methods. Total protein from each fraction was then precipitated and analyzed by Western blotting for the presence of trimers or other multimers. Presumptive dimeric and trimeric forms of MA were seen in both membrane-free (Fig. 6, lanes 1 and 2) and membrane-containing (Fig. 6, lanes 6 to 8) gradient fractions. Higher-order multimers were also apparent. Interestingly, the cross-linked membrane fractions demonstrated decreased mobility compared with the membrane-free protein, suggesting that cross-linking had revealed a difference in MA conformation in the membrane-bound form of the protein. Alternatively, cross-linking to lipids or to a small molecule located on the membrane may explain the altered mobility of the membrane-bound MA protein.

Membrane-bound and membrane-free forms of MA exist in an infected T-cell line. The experiments described above were all performed in a transient expression assay in which MA was

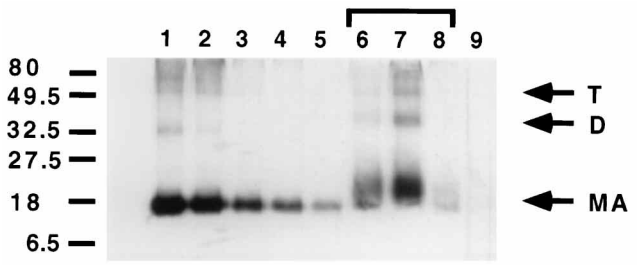

FIG. 6. Glutaraldehyde cross-linking of membrane-free MA and membrane-bound MA. The HIV-1 MA protein was produced in BSC-40 cells and subjected to equilibrium flotation centrifugation as described in Materials and Methods. Equal fractions were collected, treated with 1% glutaraldehyde, precipitated with TCA, and analyzed via SDS-PAGE and immunoblotting with an anti-MA monoclonal antibody. The molecular masses (in kilodaltons) of markers are indicated to the left. The bracket indicates gradient fractions surrounding the 65%-10% sucrose interface. D, MA dimer; T, MA trimer.

expressed at high levels. Although the harvesting of cells at an early time point (8.5 h posttransfection in the experiments shown in Fig. 3) was designed to minimize artifacts associated with overexpression of MA, it remained possible that high expression levels had produced a membrane-free form of MA which does not exist in infected cells. Therefore, we next asked if membrane-free and membrane-bound forms of MA are present in HIV-infected cells. The chronically infected cell line H9/IIIB was subjected to lysis and equilibrium flotation centrifugation as previously described, and the MA distribution in the resulting gradient fractions was assessed by immunoblotting. Membrane-bound and membrane-free forms of MA were readily identified (Fig. 7). Although the relative proportion of membrane-bound MA revealed by this analysis is larger than that demonstrated in Fig. 3A, this experiment suggests the existence of free MA in infected cells and emphasizes the importance of understanding the nature of the difference between the two fractions.

Deletions within the central globular core of MA increase membrane binding. A panel of MA protein deletion constructs has been previously constructed in the laboratory of Max Essex and assessed for production of HIV particles, envelope incorporation, and infectivity (39, 40). This panel consists of the HXB2 MA coding sequence with in-frame deletions of 10 to 14 codons spanning MA protein residues 11 to 128. A schematic diagram of the deletions and their relationship with the five alpha helices in the crystal structure of MA is shown in Fig. 1. The 10 deletion constructs were adapted for expression in the vaccinia virus/T7 system and designated MAD-1 to MAD-10

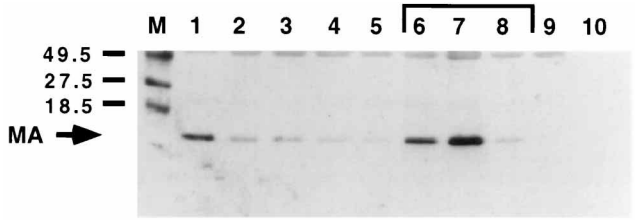

FIG. 7. Equilibrium flotation centrifugation of MA in H9/IIIB cells. Cells (10^6) of the chronically infected line H9/IIIB were harvested, lysed in hypotonic buffer by Dounce homogenization, and treated as described for BSC-40 cells prior to equilibrium flotation centrifugation. Fractions were immunoprecipitated with sera from HIV patients and analyzed via immunoblotting with an anti-MA monoclonal antibody. The molecular masses of markers are indicated in kilodaltons (lane M). The bracket indicates fractions at the membrane-containing sucrose interface.

(corresponding to D1 to D10 in the original publications). All of the constructs tested contained an intact myristyl acceptor glycine 2 residue. The rationale for analyzing this panel for membrane binding by using the flotation assay was twofold: (i) to identify internal regions essential to membrane binding of myristylated MA through a loss-of-binding phenotype and (ii) to determine if disruption of alpha-helical structure regions in the globular core of MA would enhance or inhibit myristate-mediated membrane interactions. In addition, the potential role of the C-terminal helix (helix 5) in influencing membrane interactions could be investigated.

The results of membrane flotation assays with the 10 MA deletion constructs are shown in Fig. 8. No internal deletion eliminated membrane binding of MA. Surprisingly, all deletions within the globular domain of MA, with the single exception of MAD-2, enhanced membrane binding compared with wild-type MA (Fig. 8A, C, D, E, F, and G). Each of these deletions disrupts regions of alpha helices 1 to 4 of the globular head of the molecule (outlined in Fig. 1). The globular domain deletions each resulted in 100% binding of MA to membranes. Deletions on the C-terminal tail of MA enhanced membrane association slightly (40 to 45% membrane binding versus 33% for wild-type MA as determined by densitometry of the autoradiograms shown in Fig. 8I and J). Deletion construct MAD-8 demonstrated an intermediate phenotype (Fig. 8H). Deletion construct MAD-2, which includes a deletion of the highly basic nuclear localization signal region of the molecule, demonstrated a membrane versus cytosolic distribution of MA which was indistinguishable from that of wild-type MA.

We next performed a differential sedimentation assay to verify that the deletions within the globular domain of MA had increased membrane association of the molecule. As shown in Fig. 9, the distribution of each of the deletion constructs noted in the flotation assay was verified by differential sedimentation centrifugation. The analysis in this experiment was performed by immunoblotting rather than with a pulse label; the similarities between the results obtained with these two methods indicate that the distribution of membrane versus cytosolic MA did not change significantly with time. The striking difference in distribution of the C-terminal mutants (9 and 10 in Fig. 9, demonstrating membrane-free MA and membrane-bound MA) versus the central deletions (1, 3, 4, 5, 6, and 7 in Fig. 9, all 100% membrane bound) was also observed by this method, confirming the results of the flotation assay.

Deletions which alter MA membrane versus cytosolic distribution do not alter the stability of the membrane interaction. To determine if the deletion mutations which altered the membrane binding of MA had disrupted the stability of the membrane interaction, the membrane fractions from a first flotation gradient of cell lysates expressing MAD-2, MAD-4, and MAD-5 were adjusted to 1 M NaCl prior to loading on the bottom of a second flotation gradient. Gradient fractions were collected, immunoprecipitated with sera from HIV patients, and analyzed by Western blotting with an anti-MA monoclonal antibody. No protein was dissociated from the cellular membranes by this treatment (Fig. 10). Significantly, the MAD-2 deletion construct, in which most of the positively charged residues exposed on the putative membrane-binding interface of the molecule have been deleted, remained membrane associated (Fig. 10A). Membrane interactions of all other myristylated deletion constructs were also stable as assessed in this manner (data not shown). The interaction of the MA deletion mutants with membranes in this way resembled the stability of wild-type MA (Fig. 3B) or of $Pr55^{Gag}$ (Fig. 2, bottom autoradiogram).

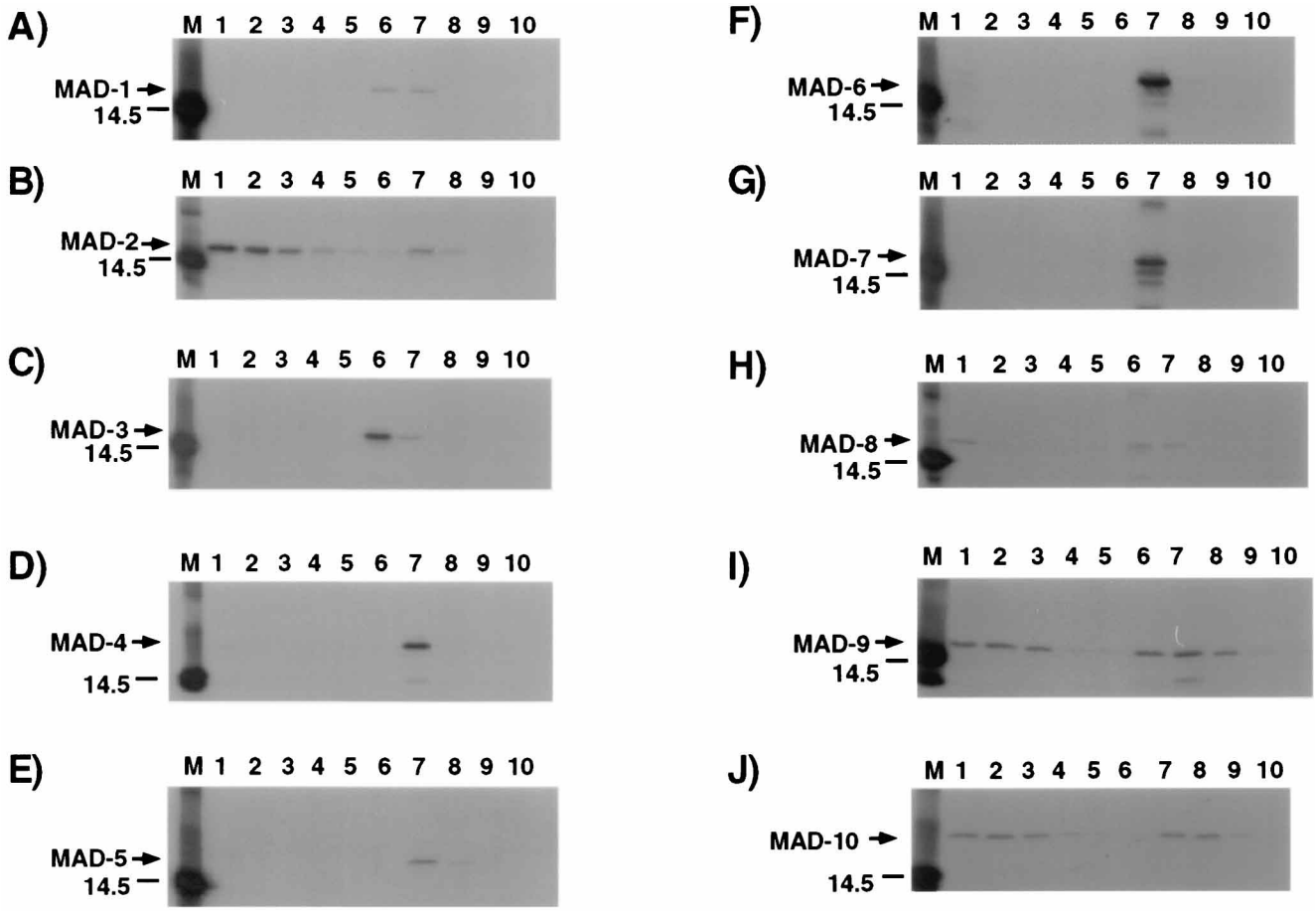

FIG. 8. Equilibrium flotation centrifugation of an MA protein deletion mutant panel. The panel of 10 MA protein deletion constructs depicted in Fig. 1 (designated pMAD1 to pMAD10) was produced in BSC-40 cells, labelled with [^{3}H]leucine, and analyzed exactly as described in the legend to Fig. 3A. The position of a 14.5-kDa marker band is indicated on each autoradiogram. Fractions 6, 7, and 8 represent the membrane-containing fractions in these experiments. A, MAD-1; B, MAD-2; C, MAD-3; D, MAD-4; E, MAD-5; F, MAD-6; G, MAD-7; H, MAD-8; I, MAD-9; J, MAD-10.

Specificity of membrane binding is determined by downstream domains of Pr55^{Gag}. The membrane flotation procedure does not discriminate between protein binding to intracellular membranes and protein binding to the plasma membrane. We therefore considered the possibility that the MA deletion constructs which demonstrate enhanced membrane binding may bind to intracellular membranes. To examine the subcellular distribution of wild-type and mutant Gag proteins in this study, we performed immunofluorescence microscopy by using monoclonal antibodies to MA. The cells were prepared for microscopy 7 h posttransfection, a time point chosen to reflect the same distribution as that used in the labelling and flotation experiments. Wild-type MA was found in a perinuclear and cytoplasmic distribution (Fig. 11A). Very little plasma membrane staining was observed. After 24 h, some plasma membrane staining was evident but the pattern remained predominantly intracellular (data not shown). MA deletion construct MAD-1 also demonstrated primarily intracellular staining, with a predominant bright perinuclear halo (Fig. 11B). The MA deletion constructs which demonstrated 100% membrane binding on flotation analysis (MAD-3, -4, -5, -6, and -7) exhibited an intracellular pattern similar to that of pMAD-1 (data not shown). In contrast, the perinuclear membranous staining was absent for Myr-MA, which exhibited a diffuse cytoplasmic distribution (Fig. 11C). Expression of Pr55^{Gag} yielded a stippled appearance which outlined the plasma membrane of the cells (Fig. 11D). This peripheral plasma membrane staining pattern was made more prominent when the focal plane was moved to the attachment site of the cell on the cover glass (Fig. 12A). Nonmyristylated Pr55^{Gag} exhibited a diffuse cytoplasmic distribution which was indistinguishable from that of Myr-MA (Fig. 12B). The difference in staining pattern between myristylated Pr55^{Gag} (Fig. 11D and 12A) and myristylated MA (Fig. 11A) indicates that domains within Pr55^{Gag} but downstream from MA contribute to specific transport to the plasma membrane.

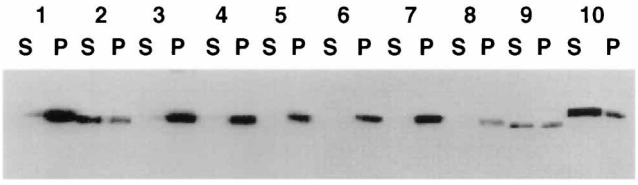

FIG. 9. Differential sedimention of an MA protein deletion mutant panel. The panel of 10 MA protein deletion constructs depicted in Fig. 1 was produced in BSC-40 cells and subjected to differential sedimentation with membranes as described in the text. Analysis was performed via immunoblotting with an anti-MA monoclonal antibody. Numbers 1 to 10 correspond to constructs MAD-1 to MAD-10. S, soluble (cytosolic) fraction; P, pellet (membrane-enriched) fraction.

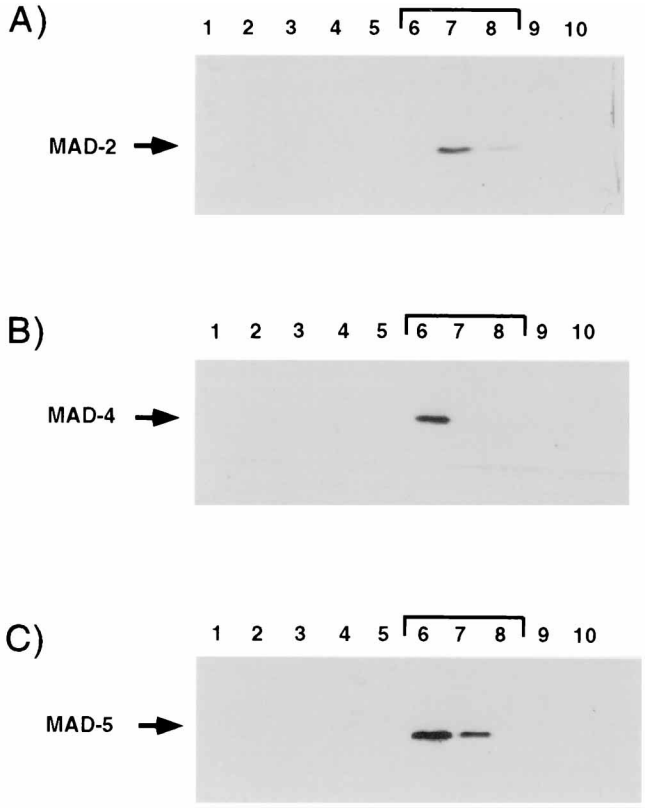

FIG. 10. Membrane binding of MA deletion constructs following exposure to 1 M NaCl. Peak membrane fractions from equilibrium flotation centrifugation of mutant MA proteins were pooled, adjusted to 1 M NaCl, and subjected to a second equilibrium centrifugation procedure. Equal fractions were then collected, immunoprecipitated with sera from HIV patients, and detected via immunoblotting with an anti-MA monoclonal antibody. The sucrose density interface containing the cellular membrane fractions is indicated by the bracket. A, MA deletion construct 2 (MAD-2); B, MA deletion construct 4 (MAD-4); C, MA deletion construct 5 (MAD-5).

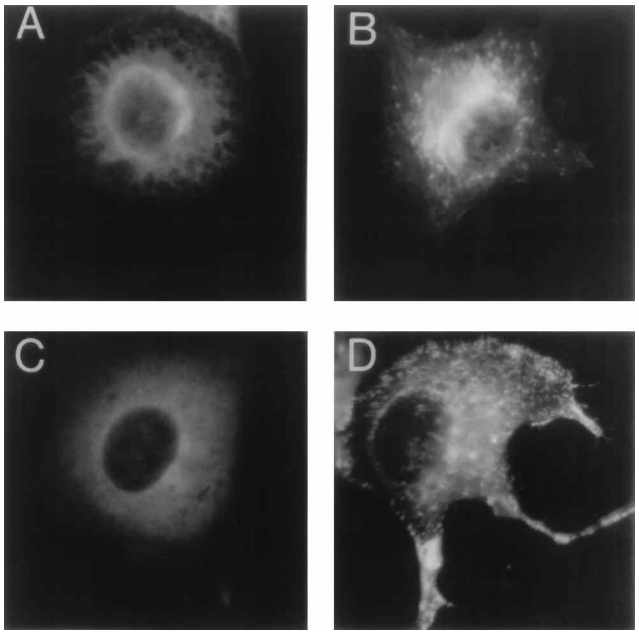

FIG. 11. Subcellular localization of HIV Gag proteins by immunofluorescence microscopy. Anti-MA monoclonal antibodies were employed to detect Gag proteins 7 h posttransfection in BSC-40 cells. Cells were photographed under a 100× oil immersion objective. A, wild-type MA; B, MAD-1; C, Myr-MA; D, $Pr55^{Gag}$.

DISCUSSION

Proteins which are modified by myristic acid may interact with cellular membranes in a reversible manner. Members of the myristylated, alanine-rich C kinase substrate (MARCKS) family of proteins interact with the plasma membrane in a manner which is reversible upon phosphorylation of the molecule (1, 2). The Arf family of proteins demonstrates myristate-mediated membrane binding which is regulated by the binding of GTP (4). Recoverin is a retinal calcium-binding protein which binds membranes in a myristate- and calcium-dependent manner (3, 35). Remarkably, this protein, when free of calcium, demonstrates sequestration of the myristyl group within a deep hydrophobic pocket as revealed by nuclear magnetic resonance spectroscopy. The crystal structure of single-Ca^{2+}-bound recoverin is markedly different, and this difference in conformation is thought to expose myristate and enhance membrane association. The importance of a reversible mechanism of membrane binding for HIV-1 MA lies in its dual role in the viral life cycle. During particle assembly, domains within MA mediate tight interaction with the plasma membrane. Following entry of the viral particle into a newly infected cell, MA must dissociate from the membrane to participate in the nuclear translocation of the preintegration complex. Our results support the hypothesis that the interaction of HIV-1 MA with cellular membranes is regulated by a conformational myristyl switch mechanism. According to this hypothesis, myristate is available for membrane interaction when in the context of $Pr55^{Gag}$. Following cleavage by the viral protease, myristate remains accessible to the membrane in a proportion of MA molecules while others undergo a conformational change which sequesters myristate and leads to membrane dissociation.

The myristyl switch mechanism: myristate is sequestered by the globular head of the molecule. The myristyl switch hypothesis, in which myristate is sequestered within MA and unavailable for membrane binding, has recently been proposed by Zhou and Resh (43). Those investigators proposed that sequestration of myristate within MA explains the difference in degree of membrane binding seen in vitro and in vivo when MA is compared to $Pr55^{Gag}$. Our results support this hypothesis. The results shown in Fig. 7 and corroborated by those in Fig. 8 offer clear evidence that disruption of alpha-helical segments of the molecule increases membrane binding dramatically. Because nonmyristylated MA does not bind cellular membranes in vivo (Fig. 3C), the simplest explanation for these findings is that myristate has been made accessible for membrane interaction by deletions located within the globular head of the molecule. Deletions located in the C-terminal tail of the molecule (exemplified by pMAD-9 and pMAD-10) increased the proportion of membrane-bound MA to a small degree but did not demonstrate the dramatic phenotype of MAD-1, -3, -4, -5, -6, and -7. Thus, we propose that the hydrophobic interactions between the tightly packed alpha helices within the globular domain of MA act to sequester myristic acid.

Although consistent with the myristyl switch hypothesis, our results regarding the important region of the molecule involved in sequestration of MA differ from those of Zhou and Resh. After using a fusion protein approach, those investigators concluded that the last alpha helix, rather than the globular head of the molecule, is the primary regulator of myristate

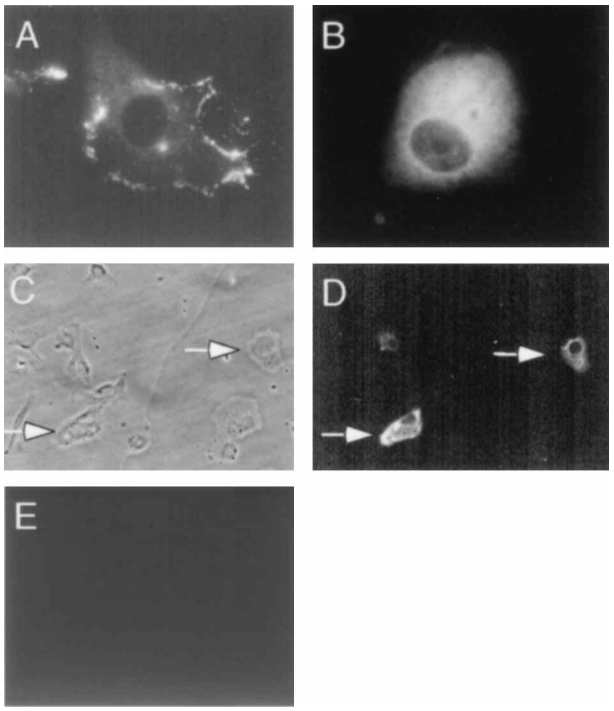

FIG. 12. Subcellular localization of HIV Gag proteins and control immunofluorescence panels. Anti-MA monoclonal antibodies were employed to detect Gag proteins in BSC-40 cells. (A) $Pr55^{Gag}$ examined with a 100× objective (magnification, ×1,000); the focal plane is at the level of contact with the coverslip. (B) Myr-$Pr55^{Gag}$ examined with a 100× objective. (C) Control panel of BSC-40 cells examined by phase-contrast microscopy using a 40× objective. (D) Same field as in C examined by immunofluorescence microscopy. Arrows indicate cells expressing Myr-$Pr55^{Gag}$. (E) Control panel of untransfected BSC-40 cells examined by immunofluorescence microscopy.

sequestration. In contrast, our results clearly demonstrate that disruption of helix 1, 2, 3, or 4 can increase membrane binding. One explanation for the discrepant findings is that the addition of dihydrofolate reductase, green fluorescent protein, or β-galactosidase to the C terminus of MA in the studies of Zhou and Resh may have altered the structure of the globular head of MA. This might allow increased binding to liposomes in a manner similar to the in vivo increase in membrane binding we found with deletions in more N-terminal regions. The fusion of heterologous proteins to the C terminus of MA in their studies may thus have acted in a manner analogous to that of downstream sequences of $Pr55^{Gag}$ to allow accessibility of myristate (discussed below).

We found that the membrane-bound MA deletion mutants were not dissociated upon treatment with 1 M NaCl or by the processing associated with a second flotation centrifugation step, a finding similar to that seen with the membrane-bound portion of wild-type MA or of $Pr55^{Gag}$. This finding is consistent with the hypothesis that myristate is the dominant membrane-interacting determinant for Gag molecules and establishes that once myristate is accessible and inserted into the membrane, the interaction is stable.

Regions of $Pr55^{Gag}$ outside of MA promote the release or membrane accessibility of myristate. Regions within $Pr55^{Gag}$ but downstream from MA clearly alter the efficiency of membrane binding, as seen in this study (Fig. 2 versus Fig. 3A) and others (27, 34, 43). According to the myristyl switch hypothesis, these downstream regions promote the accessibility of the myristate molecule to the membrane. Consistent with this, an in vitro membrane-binding study concluded that a seven-amino-acid sequence located between the two zinc finger motifs of the NC region allows appropriate exposure of the membrane-binding domain within MA and thus facilitates membrane interaction (27). How might such a downstream sequence alter the membrane-binding properties of the MA region? We propose two possible mechanisms. First, the influence of the downstream regions of $Pr55^{Gag}$ may directly promote an open configuration of the globular head domain of the MA region, with the exposure of myristate. Upon cleavage of $Pr55^{Gag}$, the molecule rearranges and myristate may be sequestered within the hydrophobic interior. Within a viral particle, some MA molecules which are stabilized by organized MA-MA interactions at the membrane may remain in the open or myristate-accessible configuration and thus remain attached to the membrane; others may assume a closed conformation which sequesters myristate and become dissociated from the membrane. The second proposed mechanism is that the downstream regions of Gag perform this function indirectly, by contributing to efficient plasma membrane transport of the precursor protein. At the plasma membrane, specific conditions or molecules exist which promote a conformational change and the exposure of myristate. The latter hypothesis would explain the specificity of the interaction of $Pr55^{Gag}$ with the plasma membrane at the exclusion of other cellular membranes. As shown by the subcellular localization data in Fig. 11 and 12, domains outside of MA are required for the typical stippled plasma membrane appearance of HIV Gag proteins examined by immunofluorescence microscopy. Accessibility of myristate itself, as proposed for MA deletion mutant MAD-1, allows tight membrane binding but not efficient plasma membrane transport (Fig. 11B). It is not clear whether downstream Gag domains participate directly in transport or promote the accessibility of both myristate and plasma membrane transport signals contained within MA.

The N-terminal basic region of MA is not required for stable membrane interaction. Our results do not support the hypothesis that electrostatic interactions between positively charged residues clustered around the mixed beta sheet of the MA structure and phospholipid head groups are essential for a stable MA-membrane interaction. Specifically, deletion of these residues (deleted in MAD-2) did not abrogate the salt-resistant binding of this protein with membranes (Fig. 10A). Consistent with this finding is the fact that this deletion did not diminish viral particle production when studied in the context of a proviral clone (40). However, other investigators have demonstrated the contribution of charged residues within this region to membrane binding in in vitro binding assays (42). It should be noted that the MAD-2 deletion eliminates lysines 24, 26, and 30 but does not remove lysine 32 or charged residues which are proximal to this region (Lys-18 and Arg-20). Thus, although the residues in the deleted region clearly are not essential for the salt-resistant, myristylation-dependent binding of MA, it is possible that the remaining charged residues contributed to membrane binding through interactions with membrane phospholipids.

MA oligomers may be membrane free or membrane bound in vivo. HIV-1 MA can oligomerize in solution (33), and the crystal structure of MA reveals a trimeric complex (20). The contribution of MA trimerization to assembly events or postentry events in the virus life cycle is not known. The developing particle includes approximately 2,000 Gag protein molecules (26), which multimerize primarily due to the influence of domains located in the C-terminal portion of CA and the N-terminal portion of NC (13). Presumably, MA participates in the formation of higher-order multimers during as-

sembly and remains as an icosahedral shell on the inner surface of the lipid bilayer of the particle following cleavage by the HIV protease (25). This process has been modeled for simian immunodeficiency virus MA (28). We show for the first time that MA may form dimers, trimers, and higher-order oligomers when expressed within cells and that oligomeric forms of MA may be membrane bound or membrane free (Fig. 6). Thus, oligomerization does not require membrane binding, nor does it preclude it. Our data do not establish whether certain oligomeric forms (such as trimers) of MA are enhanced in their membrane interaction compared to monomers, which will be a subject of interest in future studies. Interestingly, cross-linking of MA which was bound to membranes reduced the mobility of MA monomers, dimers, and trimers upon separation by SDS-PAGE. We interpret this as evidence in favor of the existence of an altered membrane-bound conformation of MA which has been stabilized by the cross-linking procedure. Such a conformational change to a myristate-accessible conformation remains to be directly proven. Alternatively, it is possible that a small molecule was cross-linked with MA or that MA-lipid cross-linking resulted in its slower migration.

The role of phosphorylation in membrane binding. The regulator of a myristyl switch mechanism for HIV MA remains to be conclusively identified. Several studies have concluded that phosphorylation of MA regulates its membrane association (6, 8, 17, 18, 38). It has been proposed that the addition of negative charges through phosphorylation events can negate the electrostatic interactions occurring at the inner plasma membrane surface between positively charged MA residues and the lipid bilayer and dissociate MA from this membrane (6). The data are conflicting, however. One line of evidence has revealed that phosphorylation of MA on residue S^{111} by protein kinase C was essential for the membrane-binding properties of MA (38). Others, including workers in our laboratory, have been unable to demonstrate this requirement by using site-directed mutation of S^{111} and subcellular fractionation techniques (33, 43). Phosphorylation of MA occurring within virion particles has also been demonstrated to mediate membrane dissociation and promote nuclear import of MA. This inhibition of membrane binding may occur due to phosphorylation on both tyrosine and serine residues (6) or on a specific C-terminal tyrosine residue alone (Y^{132}) (17). The present study establishes that phosphorylation of MA does not of itself result in a shift to a membrane-bound or a membrane-free state. The distribution of phosphorylated MA shown in Fig. 5B mirrors the distribution of total MA within the cell. Whether phosphorylation on specific residues may alter the conformation of MA and result in the myristate-accessible form of MA or the myristate-sequestered form is not answered by this work but will be addressed in future studies by phosphoamino acid analysis and tryptic digest mapping of phosphorylated protein in membrane-bound versus membrane-free fractions.

In summary, our results support a myristyl switch mechanism which regulates the reversible membrane binding of MA. The tightly packed alpha helices of the globular head of the molecule contribute to the sequestering of myristate in a significant proportion of MA molecules. It will be important to identify the precise trigger of the Gag protein myristyl switch to understand the means by which HIV Gag proteins can reversibly interact with membranes and perform multiple functions in the life cycle of HIV.

ACKNOWLEDGMENTS

P.S. is an AMFAR scholar (award 70422-15-RF) and was supported by NIH-NIAID N01-A1-45210 and a Child Health Research Center grant. L.R. is an American Cancer Society Research Professor and was supported by Public Health Service grants.

We thank Max Essex and coworkers for providing MA deletion constructs D1 to D10, A. Pinter for providing anti-MA monoclonal antibodies, and Chris Aiken and Barney Graham for critically reviewing the manuscript.

REFERENCES

1. **Aderem, A.** 1992. The MARCKS brothers: a family of protein kinase C substrates. Cell **71:**713–716.
2. **Aderem, A.** 1992. The role of myristoylated protein kinase C substrates in intracellular signaling pathways in macrophages. Curr. Top. Microbiol. Immunol. **181:**189–207.
3. **Ames, J. B., T. Tanaka, L. Stryer, and M. Ikura.** 1994. Secondary structure of myristoylated recoverin determined by three-dimensional heteronuclear NMR: implications for the calcium-myristoyl switch. Biochemistry **33:**10743–10753.
4. **Boman, A. L., and R. A. Kahn.** 1995. Arf proteins: the membrane traffic police? Trends Biochem. Sci. **20:**147–150.
5. **Bryant, M., and L. Ratner.** 1990. Myristoylation-dependent replication and assembly of human immunodeficiency virus 1. Proc. Natl. Acad. Sci. USA **87:**523–527.
6. **Bukrinskaya, A. G., A. Ghorpade, N. K. Heinzinger, T. E. Smithgall, R. E. Lewis, and M. Stevenson.** 1996. Phosphorylation-dependent human immunodeficiency virus type 1 infection and nuclear targeting of viral DNA. Proc. Natl. Acad. Sci. USA **93:**367–371.
7. **Bukrinsky, M. I., S. Haggerty, M. P. Dempsey, N. Sharova, A. Adzhubel, L. Spitz, P. Lewis, D. Goldfarb, M. Emerman, and M. Stevenson.** 1993. A nuclear localization signal within HIV-1 matrix protein that governs infection of non-dividing cells. Nature **365:**666–669.
8. **Burnette, B., G. Yu, and R. L. Felsted.** 1993. Phosphorylation of HIV-1 gag proteins by protein kinase C. J. Biol. Chem. **268:**8698–8703.
9. **Carrillo, A., and L. Ratner.** 1996. Human immunodeficiency virus type 1 tropism for T-lymphoid cell lines: role of the V3 loop and C4 envelope determinants. J. Virol. **70:**1301–1309.
10. **Chong, L. D., and J. K. Rose.** 1994. Interactions of normal and mutant vesicular stomatitis virus matrix proteins with the plasma membrane and nucleocapsids. J. Virol. **68:**441–447.
11. **Chong, L. D., and J. K. Rose.** 1993. Membrane association of functional vesicular stomatitis virus matrix protein in vivo. J. Virol. **67:**407–414.
12. **Dorfman, T., F. Mammano, W. A. Haseltine, and H. G. Gottlinger.** 1994. Role of the matrix protein in the virion association of the human immunodeficiency virus type 1 envelope glycoprotein. J. Virol. **68:**1689–1696.
13. **Franke, E. K., H. E. Yuan, K. L. Bossolt, S. P. Goff, and J. Luban.** 1994. Specificity and sequence requirements for interactions between various retroviral Gag proteins. J. Virol. **68:**5300–5305.
14. **Freed, E. O., G. Englund, and M. A. Martin.** 1995. Role of the basic domain of human immunodeficiency virus type 1 matrix in macrophage infection. J. Virol. **69:**3949–3954.
15. **Freed, E. O., and M. A. Martin.** 1995. Virion incorporation of envelope glycoproteins with long but not short cytoplasmic tails is blocked by specific, single amino acid substitutions in the human immunodeficiency virus type 1 matrix. J. Virol. **69:**1984–1989.
16. **Gallay, P., V. Stitt, C. Mundy, M. Oettinger, and D. Trono.** 1996. Role of the karyopherin pathway in human immunodeficiency virus type 1 nuclear import. J. Virol. **70:**1027–1032.
17. **Gallay, P., S. Swingler, C. Aiken, and D. Trono.** 1995. HIV-1 infection of nondividing cells: C-terminal tyrosine phosphorylation of the viral matrix protein is a key regulator. Cell **80:**379–388.
18. **Gallay, P., S. Swingler, J. Song, F. Bushman, and D. Trono.** 1995. HIV nuclear import is governed by the phosphotyrosine-mediated binding of matrix to the core domain of integrase. Cell **83:**569–576.
19. **Gottlinger, H. G., J. G. Sodroski, and W. A. Haseltine.** 1989. Role of capsid precursor processing and myristoylation in morphogenesis and infectivity of human immunodeficiency virus type 1. Proc. Natl. Acad. Sci. USA **86:**5781–5785.
20. **Hill, C. P., D. Worthylake, D. P. Bancroft, A. M. Christensen, and W. I. Sundquist.** 1996. Crystal structures of the trimeric human immunodeficiency virus type 1 matrix protein: implications for membrane association and assembly. Proc. Natl. Acad. Sci. USA **93:**3099–3104.
21. **Karacostas, V., K. Nagashima, M. A. Gonda, and B. Moss.** 1989. Human immunodeficiency virus-like particles produced by a vaccinia virus expression vector. Proc. Natl. Acad. Sci. USA **86:**8964–8967.
22. **Mergener, K., M. Facke, R. Welker, V. Brinkmann, H. R. Gelderblom, and H. G. Krausslich.** 1992. Analysis of HIV particle formation using transient expression of subviral constructs in mammalian cells. Virology **186:**25–39.
23. **Morikawa, Y., T. Kishi, W. H. Zhang, M. V. Nermut, D. J. Hockley, and I. M. Jones.** 1995. A molecular determinant of human immunodeficiency virus particle assembly located in matrix antigen p17. J. Virol. **69:**4519–4523.
24. **Moss, B., O. Elroy-Stein, T. Mizukami, W. A. Alexander, and T. R. Fuerst.**

1990. Product review. New mammalian expression vectors. Nature **348:**91–92.
25. **Nermut, M. V., C. Grief, S. Hashmi, and D. J. Hockley.** 1993. Further evidence of icosahedral symmetry in human and simian immunodeficiency virus. AIDS Res. Hum. Retroviruses **9:**929–938.
26. **Nermut, M. V., D. J. Hockley, J. B. Jowett, I. M. Jones, M. Garreau, and D. Thomas.** 1994. Fullerene-like organization of HIV gag-protein shell in virus-like particles produced by recombinant baculovirus. Virology **198:**288–296.
27. **Platt, E. J., and O. K. Haffar.** 1994. Characterization of human immunodeficiency virus type 1 Pr55gag membrane association in a cell-free system: requirement for a C-terminal domain. Proc. Natl. Acad. Sci. USA **91:**4594–4598.
28. **Rao, Z., A. S. Belyaev, E. Fry, P. Roy, I. M. Jones, and D. I. Stuart.** 1995. Crystal structure of SIV matrix antigen and implications for virus assembly. Nature **378:**743–747.
29. **Ratner, L., A. Fisher, L. L. Jagodzinski, H. Mitsuya, R. S. Liou, R. C. Gallo, and F. Wong-Staal.** 1987. Complete nucleotide sequences of functional clones of the AIDS virus. AIDS Res. Hum. Retroviruses **3:**57–69.
30. **Rose, J. K., L. Buonocore, and M. A. Whitt.** 1991. A new cationic liposome reagent mediating nearly quantitative transfection of animal cells. BioTechniques **10:**520–525.
31. **Royer, M., S. S. Hong, B. Gay, M. Cerutti, and P. Boulanger.** 1992. Expression and extracellular release of human immunodeficiency virus type 1 Gag precursors by recombinant baculovirus-infected cells. J. Virol. **66:**3230–3235.
32. **Shang, F., H. Huang, K. Revesz, H.-C. Chen, R. Herz, and A. Pinter.** 1991. Characterization of monoclonal antibodies against the human immunodeficiency virus matrix protein, $p17^{gag}$: identification of epitopes exposed at the surfaces of infected cells. J. Virol. **65:**4798–4804.
33. **Spearman, P.** Unpublished observations.
34. **Spearman, P., J. J. Wang, N. Vander Heyden, and L. Ratner.** 1994. Identification of human immunodeficiency virus type 1 Gag protein domains essential to membrane binding and particle assembly. J. Virol. **68:**3232–3242.
35. **Tanaka, T., J. B. Ames, T. S. Harvey, L. Stryer, and M. Ikura.** 1995. Sequestration of the membrane-targeting myristoyl group of recoverin in the calcium-free state. Nature **376:**444–447.
36. **von Schwedler, U., R. S. Kornbluth, and D. Trono.** 1994. The nuclear localization signal of the matrix protein of human immunodeficiency virus type 1 allows the establishment of infection in macrophages and quiescent T lymphocytes. Proc. Natl. Acad. Sci. USA **91:**6992–6996.
37. **Wills, J. W., and R. C. Craven.** 1991. Form, function, and use of retroviral gag proteins. AIDS **5:**639–654. (Editorial.)
38. **Yu, G., F. S. Shen, S. Sturch, A. Aquino, R. I. Glazer, and R. L. Felsted.** 1995. Regulation of HIV-1 gag protein subcellular targeting by protein kinase C. J. Biol. Chem. **270:**4792–4796.
39. **Yu, X., Q. C. Yu, T. H. Lee, and M. Essex.** 1992. The C terminus of human immunodeficiency virus type 1 matrix protein is involved in early steps of the virus life cycle. J. Virol. **66:**5667–5670.
40. **Yu, X., X. Yuan, Z. Matsuda, T. H. Lee, and M. Essex.** 1992. The matrix protein of human immunodeficiency virus type 1 is required for incorporation of viral envelope protein into mature virions. J. Virol. **66:**4966–4971.
41. **Yuan, X., X. Yu, T. H. Lee, and M. Essex.** 1993. Mutations in the N-terminal region of human immunodeficiency virus type 1 matrix protein block intracellular transport of the Gag precursor. J. Virol. **67:**6387–6394.
42. **Zhou, W., L. J. Parent, J. W. Wills, and M. D. Resh.** 1994. Identification of a membrane-binding domain within the amino-terminal region of human immunodeficiency virus type 1 Gag protein which interacts with acidic phospholipids. J. Virol. **68:**2556–2569.
43. **Zhou, W., and M. D. Resh.** 1996. Differential membrane binding of the human immunodeficiency virus type 1 matrix protein. J. Virol. **70:**8540–8548.